

Molecular-Field Theory of Phase Transitions in TbPO_4 and in TmAsO_4

Jean Sivardière

Département de Recherche Fondamentale, Centre d'Etudes Nucléaires, B.P. 85, 38041, Grenoble, France

(Received 26 February 1973)

The crystallographic and magnetic phase transitions observed in TbPO_4 and TmAsO_4 are described phenomenologically. A symmetry-adapted spin Hamiltonian, involving various dipolar and quadrupolar interactions, is constructed and treated in the molecular-field approximation. One or two phase transitions are found according to the values of the interaction parameters, and it is shown that the crystallographic distortion in the paramagnetic distorted phase is monoclinic. The results are interpreted in terms of the Pytte and Stevens model for rare-earth vanadates.

I. INTRODUCTION

Rare-earth vanadates, arsenates, and phosphates, which crystallize in the tetragonal zircon structure, exhibit interesting crystallographic and magnetic phase transitions. The crystallographic distortions observed in DyVO_4 ,¹ DyAsO_4 ,² TbVO_4 ,³ TbAsO_4 ,⁴ TmVO_4 ,⁵ and TmAsO_4 ⁶ are believed to be Jahn-Teller induced. In DyVO_4 ,¹ DyAsO_4 ,² TbVO_4 ,³ and TbAsO_4 ,⁴ a second phase transition is observed at a lower temperature and corresponds to the onset of colinear antiferromagnetic ordering in the basal plane perpendicular to the optical axis. Various theories of these successive phase transitions have been proposed recently.⁷⁻¹⁰

The properties of TbPO_4 are somewhat different.¹¹⁻¹⁵ At $T_D = 3.5^\circ\text{K}$, TbPO_4 undergoes a crystallographic distortion from tetragonal to some lower symmetry,^{13,14} orthorhombic *or* monoclinic. At $T_N = 2.2^\circ\text{K}$, antiferromagnetism appears along a direction which is *not* in the basal plane but well off the c axis in the (110) plane.^{11,15} In this paper we shall give a phenomenological description of these two successive phase transitions, using the molecular-field approximation (no sublattice structure will be introduced, since we shall not study the influence of a magnetic field). The use of this approximation is justified at least for the crystallographic distortion, since the Jahn-Teller interactions are suspected to be of a long range. We shall prove also that the distortions observed in TbPO_4 and TmAsO_4 are of the same nature.

This paper is organized as follows: In Sec. II, we discuss the symmetry of the dipolar and quadrupolar operators used to construct the spin Hamiltonian describing TbPO_4 . In Sec. III, we use a quadrupolar Hamiltonian having the restricted axial symmetry defined in Ref. 16 and we investigate the possibility of an orthorhombic distortion of the lattice followed by a magnetic transition. In Sec. IV, we study the possibility of successive orthorhombic and monoclinic distor-

tions. The two above situations, in fact, have to be rejected and in Sec. V we suppose that the distortion below T_D is monoclinic. The two transitions observed in TbPO_4 are reproduced and we look for the possibility of three successive phase transitions. In Sec. VI we discuss the properties of TmAsO_4 and compare them to those of TmVO_4 and TbPO_4 . Finally, in Sec. VII the results are interpreted in terms of the Pytte-Stevens model⁷ proposed for rare-earth vanadates.

II. DIPOLAR AND QUADRUPOLAR OPERATORS

The ion Tb^{3+} in TbPO_4 has three low-lying crystalline-field levels well separated from the excited states¹²: a non-Kramers doublet Γ_5 and a singlet Γ_α ($\alpha = 1, 2, 3$, or 4), the exact symmetry of which is not known (in fact this symmetry is likely to be Γ_1 according to elementary crystal-field calculations—see Appendix A). In the following, we shall neglect entirely the excited states, and construct an effective $S' = 1$ spin Hamiltonian.

We choose the x axis along the [110] direction, that is parallel to a twofold axis, and the z axis along the [001] direction, in agreement with Ref. 17. Since the moments are found in the (110) plane, we need to know the form of the dipolar operators S^x and S^z , and of the quadrupolar operators $(S^x)^2$, $(S^y)^2 - (S^z)^2$, and $S^x S^z + S^z S^x$. The transformation properties of these operators under the operations of the point group $D_{2d} = \bar{4}2m$ are shown in Table I (we show also the transformation properties of the spin states $|M\rangle$ for $S = 1$, and classify some isomorphous compounds according to the symmetry of their Jahn-Teller distortions or

TABLE I. Transformation properties of the dipolar and quadrupolar operators in point group $D_{2d} = \bar{4}2m$; x is parallel to the twofold axis [110].

Γ_1	A_1		$(S^x)^2 + (S^y)^2; (S^z)^2$		
Γ_2	A_2	S^z		$ 0\rangle$	$\text{DyPO}_4; \text{GdVO}_4$
Γ_3	B_1		$(S^y)^2 - (S^z)^2$		$\text{TbVO}_4; \text{TmVO}_4$
Γ_4	B_2		$S^x S^y + S^y S^x$		DyVO_4
Γ_5	E	$\begin{pmatrix} S^x \\ S^y \end{pmatrix}$	$\begin{pmatrix} S^y S^z + S^z S^y \\ -S^x S^z - S^z S^x \end{pmatrix}$	$\begin{pmatrix} +1 \rangle \\ -1 \rangle \end{pmatrix}$	$\text{TbPO}_4; \text{TmAsO}_4$

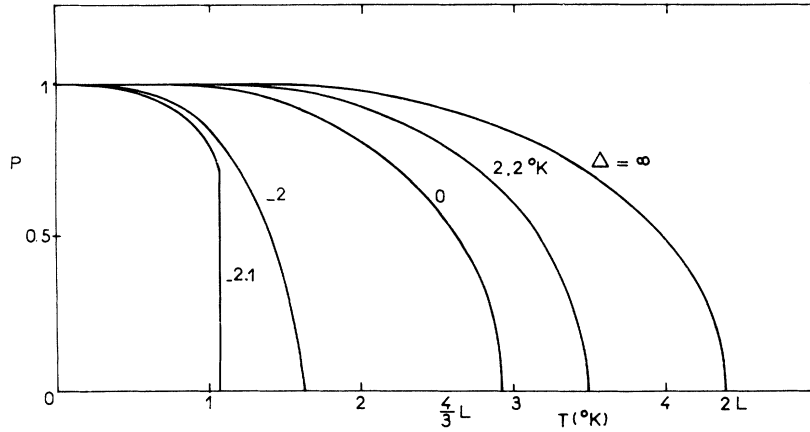


FIG. 1. Thermal variation of the parameter P according to Hamiltonian (1), for $L=2.2^\circ\text{K}$ and various values of the energy Δ .

magnetic transitions). Since $(\Gamma_5)^2 = \Gamma_1 + \Gamma_2 + \Gamma_3 + \Gamma_4$ and $\Gamma_\alpha \Gamma_5 = \Gamma_5$, we find easily the number of their matrix elements. The exact form of the operators is determined by use of orthogonality relations or by comparison to the case of a true spin $S=1$:

$$S^x = \begin{pmatrix} g_5 & & \\ & -g_5 & \\ & & 0 \end{pmatrix}, \quad S^y = \begin{pmatrix} & g_{\alpha 5} & \\ & & g_{\alpha 5} \\ g_{\alpha 5} & & g_{\alpha 5} \end{pmatrix},$$

$$(S^x)^2 = \begin{pmatrix} q_5 & & \\ & q_5 & \\ & & q_\alpha \end{pmatrix}, \quad (S^x)^2 - (S^y)^2 = \begin{pmatrix} p_5 & & \\ & & \\ p_5 & & \end{pmatrix},$$

$$S^x S^x + S^y S^y = \begin{pmatrix} & p'_{\alpha 5} & \\ p'_{\alpha 5} & & -p'_{\alpha 5} \\ & -p'_{\alpha 5} & \end{pmatrix}.$$

Because of the lack of experimental information on the coefficient g_5 , $g_{\alpha 5}$, q_5 , \dots , we shall replace the effective spin $S'=1$ by a true spin $S=1$:

$$g_5 = 1, \quad g_{\alpha 5} = 1/\sqrt{2};$$

$$q_5 = 1, \quad q_\alpha = 0;$$

$$p_5 = 1, \quad p'_{\alpha 5} = 1/\sqrt{2}.$$

III. RESTRICTED AXIAL QUADROPOLAR HAMILTONIAN

In this section we shall suppose that the distortion of the TbPO_4 lattice below T_D has the orthorhombic symmetry already observed in TbVO_4 ³ and TbAsO_4 .⁴ Neglecting first the possibility of magnetic ordering, we consider the following quadrupolar Hamiltonian:

$$\mathcal{H} = -\Delta \sum_i Q_i - \sum_{ij} L_{ij} P_i P_j, \quad (1)$$

with

$$Q_i = (S_i^x)^2$$

and

$$P_i = (S_i^x)^2 - (S_i^y)^2.$$

This Hamiltonian has the restricted axial symmetry defined in Ref. 16. For $\Delta < 0$, the situation corresponds to that of the Blume¹⁸-Capel¹⁹ model.

The molecular-field approximation will be used throughout this paper (for details see Ref. 9). The order parameter $P = (S_i^x)^2 - (S_i^y)^2$ describing the orthorhombic distortion is given by

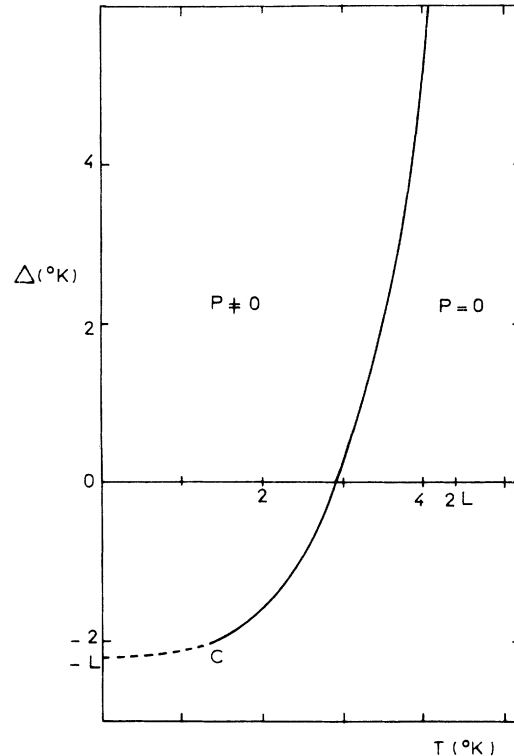


FIG. 2. Phase diagram in the (Δ, T) plane for Hamiltonian (1), $L=2.2^\circ\text{K}$. C is a tricritical point; $\Delta_c = -2.02^\circ\text{K}$ and $T_c = 1.46^\circ\text{K}$. The dashed line indicates first-order transitions.

$$P = \frac{2 \sinh 2\beta LP}{e^{-\beta\Delta} + 2 \cosh 2\beta LP}, \quad (2)$$

with $\beta = 1/KT$ and

$$L = L(0) = \sum_j L_{ij}.$$

If the transition in P is second order, the transition temperature T_P is given by

$$4\beta_P L = 2 + e^{-\beta_P L}. \quad (3)$$

If Δ is very large as in TmVO_4 ,¹⁰ $kT_P \approx 2L$; if $\Delta = 0$, $kT_P = \frac{4}{3}L$. With $T_P = 3.5^\circ\text{K}$ ¹³ and $\Delta = 2.2^\circ\text{K}$,¹² we find $L = 2.2^\circ\text{K}$.

We have performed a Landau type of development of the free energy ϕ in order to find the influence of Δ on the order of the transition:

$$\begin{aligned} \phi &= -(1/\beta) \ln(e^{-\beta\Delta} + 2 \cosh 2\beta LP) + LP^2 \\ &= \phi_0 + A(\Delta, T)P^2 + B(\Delta, T)P^4 + \dots \end{aligned} \quad (4)$$

A tricritical point C is found for $A(\Delta, T) = B(\Delta, T) = 0$, or $\beta\Delta = -\ln 4$ and $\beta L = \frac{3}{2}$. The thermal variation of P for $L = 2.2^\circ\text{K}$ and various values of Δ is represented in Fig. 1. For $-L < \Delta < \Delta_c$, the transition is first order. For $\Delta < -L$, there is no transition.

The phase diagram in the (T, Δ) plane is shown in Fig. 2. It is easy to see that the application of a magnetic field H_z hinders and eventually suppresses the orthorhombic distortion, which on the contrary is induced even at high temperatures by the application of a field H_x . The second effect should be much easier to observe in TbPO_4 than in TmVO_4 ⁵ or TmAsO_4 ,⁶ where Δ is large.

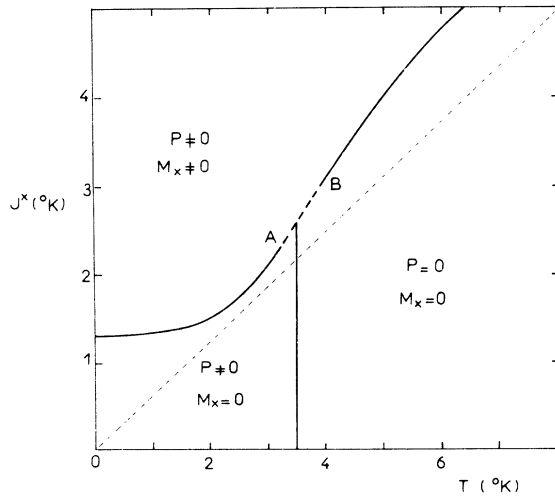


FIG. 3. Phase diagram in the (J^x, T) plane for Hamiltonian (6); $\Delta = 2.2^\circ\text{K}$ and $L = 2.2^\circ\text{K}$. A and B are tricritical points. The dashed line indicates first-order transitions. The dotted line corresponds to $\Delta = L = 0$. Then $T_{M_x} = \frac{2}{3}S(S+1)J^x = \frac{4}{3}J^x$.

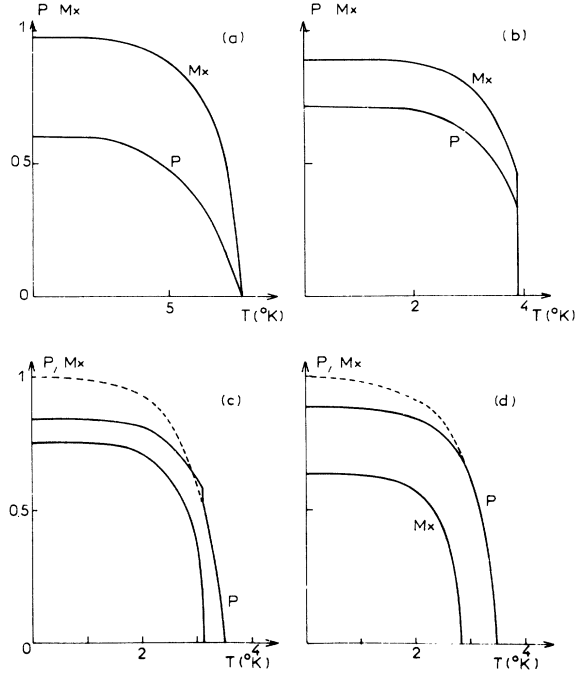


FIG. 4. Thermal variation of the parameters P and M_x according to Hamiltonian (6), $\Delta = 2.2^\circ\text{K}$ and $L = 2.2^\circ\text{K}$. (a) $J^x = 6^\circ\text{K}$; (b) $J^x = 3^\circ\text{K}$; (c) $J^x = 2.2^\circ\text{K}$; and (d) $J^x = 2^\circ\text{K}$.

We shall now introduce various dipolar interactions in the Hamiltonian (1) to see whether a dipolar phase transition may follow the orthorhombic distortion. If the dipolar interaction

$$- \sum_{ij} J_{ij}^x S_i^x S_j^x \quad (5)$$

is added to the Hamiltonian (1), the molecular-field equations for the order parameters P and $M_x = \langle S^x \rangle$ are

$$\begin{aligned} P &= \frac{4LP}{R} \frac{\sinh \beta R}{Z_0}, \\ M_x &= \frac{4J^x M_x}{R} \frac{\sinh \beta R}{Z_0}, \end{aligned}$$

with

$$R^2 = 4[L^2 P^2 + (J^x)^2 M_x^2]$$

and

$$Z_0 = e^{-\beta\Delta} + 2 \cosh \beta R.$$

(Z_0 is the molecular-field partition function.) As in the case of TmVO_4 ,¹⁰ ordering in P or M_x is found according to the value of J^x/L .

We thus now consider the Hamiltonian

$$\mathcal{H} = -\Delta \sum_i Q_i - \sum_{ij} L_{ij} P_i P_j - \sum_{ij} J_{ij}^x S_i^x S_j^x. \quad (6)$$

(We do not need to introduce dipolar interactions

along y since we shall study only domains with $P > 0$.) This Hamiltonian has already been studied by Chen and Levy²⁰ in the case when $\Delta = 0$. According to the ratio J^x/L , a single transition in $M_x = \langle S_i^x \rangle$ and P , or two successive phase transitions are found (see Fig. 3). Thermal variations of P and M_x are shown in Fig. 4 for various values of J^x . Figure 5 shows the thermal variation of the single-ion energy levels of the system in the case of two successive second-order phase transitions.

Although two phase transitions are found at $T_P = 3.5^\circ\text{K}$ and $T_{M_x} = 2.2^\circ\text{K}$ for $L = 2.2^\circ\text{K}$ and $J^x \approx 1.8^\circ\text{K}$, these results do not describe correctly the behavior of TbPO_4 , since in this compound the magnetization appears along some direction of the xz plane¹¹ and not along the x axis. (The magnetic ordering in TbPO_4 is antiferromagnetic but, as long as no magnetic field is applied, the sign of the dipolar interaction is unimportant.⁹)

We have finally added the interactions (5) to the Hamiltonian (6) and looked for ordering in the three order parameters P , M_x , and M_y . We found no solution with $M_x \neq 0$ and $M_y \neq 0$, in agreement with the discussion of Chen and Levy²⁰ who examined the case $\Delta = 0$ and $J^x = J^y$. In the second case, as noted above, there is only one phase transition in M_y : at any temperature, $P = 0$.

Consequently our hypothesis of a Hamiltonian with a restricted axial symmetry, that is of an orthorhombic distortion below T_D , leads to the

conclusion that the magnetization may appear only along x , in contradiction with the neutron-diffraction experimental results.^{11,15} We are then forced to give up this hypothesis, and in Sec. IV we examine the possibility of a monoclinic distortion, the Hamiltonian having the fully axial symmetry. Another possibility would be to introduce excited electronic levels but, according to Refs. 12 and 14, their influence is unlikely to modify the above results: Although the entropy variation between 0 and 20°K is $\Delta S \approx R \ln 4$,¹³ there are numerous excited levels above 40°K which contribute to this entropy variation, so that the value of ΔS is not the proof that a second excited singlet should be introduced. Anyway, the following sections will show that this introduction is not necessary.

IV. FULLY AXIAL QUADRUPOLAR HAMILTONIAN

A monoclinic distortion is described by the order parameters

$$P = \langle (S_i^x)^2 - (S_i^y)^2 \rangle \neq 0$$

and

$$P' = \langle S_i^x S_i^z + S_i^y S_i^z \rangle \neq 0,$$

or

$$P'' = \langle S_i^y S_i^z + S_i^x S_i^z \rangle \neq 0.$$

For instance when P' is different from zero, y is a principal axis of the quadrupoles, but the prin-

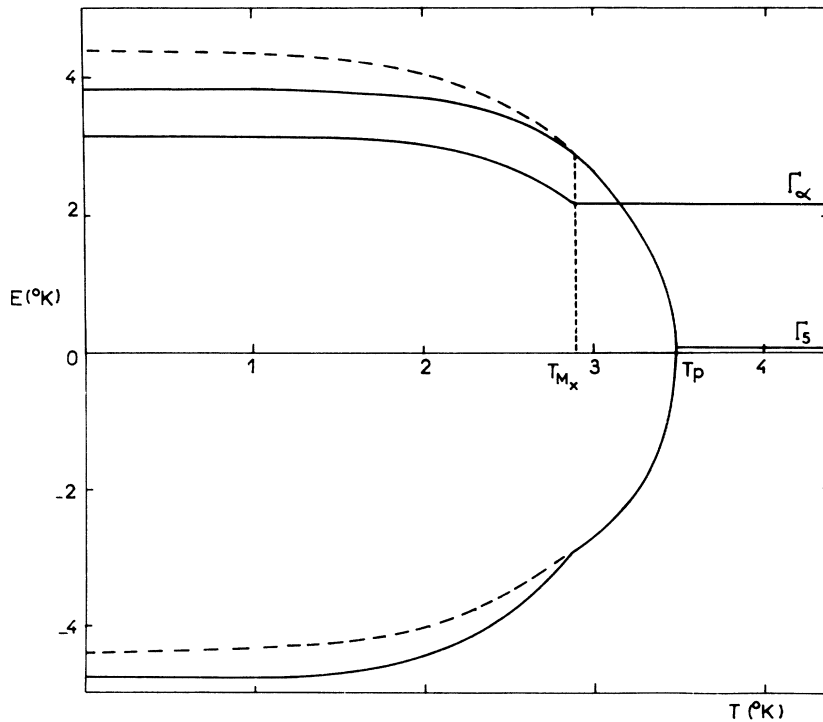


FIG. 5. Thermal variation of the single-ion energy levels according to Hamiltonian (6) for $\Delta = L = 2.2^\circ\text{K}$ and $J^x = 2^\circ\text{K}$.

principal axis in the xz plane are not the x and z axis. In fact, if $|P|$ is different from zero, P' or P'' is different from zero, and the corresponding domains differ in the sign of P . Moreover if $|P'|$ is different from zero, there are two types of domains, differing in the sign of P' . The domains $P' \leq 0$ (or $P'' \leq 0$) are analogous to magnetic anti-phase domains.

We now evaluate the angle θ between z and z' , one of the principal axes in the xz plane. Considering the components S^x , S^y , and S^z of the spin as the components X , Y , and Z of a classical vector, we have

$$\begin{aligned} Q &= Z^2, \\ P &= X^2 - Y^2, \\ 2 &= X^2 + Y^2 + Z^2, \end{aligned} \quad (7)$$

whence

$$\begin{aligned} X^2 &= \frac{1}{2}(P + 2 - Q), \\ X^2 - Z^2 &= \frac{1}{2}(P + 2 - 3Q), \\ 2XZ &= P'. \end{aligned} \quad (7a)$$

We also have

$$2X'Z' = \cos 2\theta(2XZ) - \sin 2\theta(X^2 - Z^2) = 0,$$

so that

$$\tan 2\theta = \frac{2P'}{P + 2 - 3Q}. \quad (8)$$

Let us now consider the Hamiltonian

$$\mathcal{H} = \Delta \sum_i Q_i - \sum_{ij} L_{ij} P_i P_j - \sum_{ij} L'_{ij} P'_i P'_j, \quad (9)$$

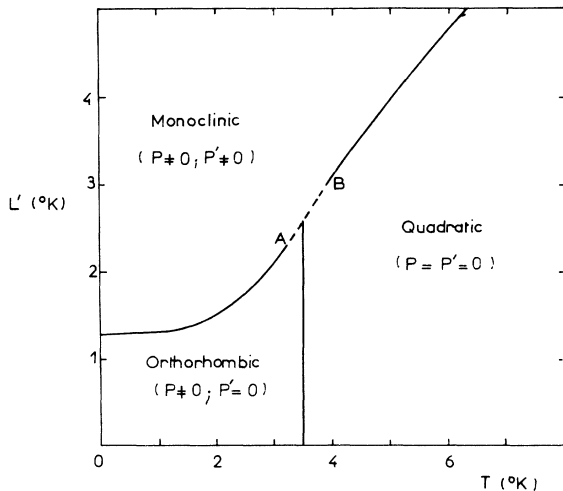


FIG. 6. Phase diagram in the (L', T) plane for Hamiltonian (9); $\Delta = 2.2^\circ\text{K}$ and $L = 2.2^\circ\text{K}$. The point symmetries of the quadratic orthorhombic and monoclinic phases are $\bar{4}2m$, $2_x 2_y 2_z$, and 2_y , respectively.

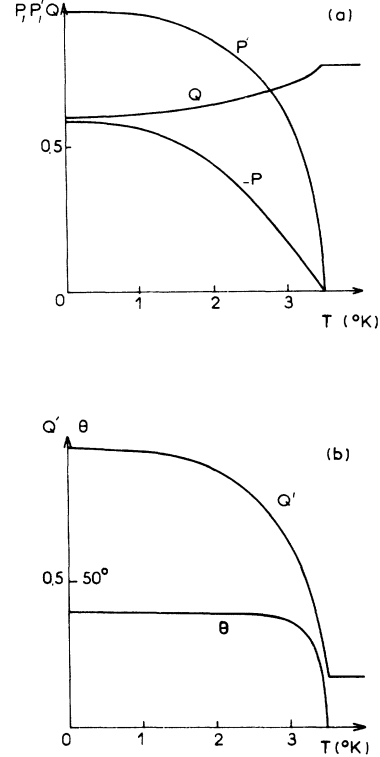


FIG. 7. Results for Hamiltonian (9) for $\Delta = 2.2^\circ\text{K}$; $L = 0$ and $L' = 3.1^\circ\text{K}$. (a) Thermal variation of P , P' , and Q ; (b) thermal variation of θ and $Q' = \langle (S_z^2)^2 - (S_x^2)^2 \rangle$.

and look for ordering in the parameters P and P' , for given values of $\Delta = 2.2^\circ\text{K}$ and $L = 2.2^\circ\text{K}$. In fact, because of the similarity between the operators S^x and $S^x S^z + S^z S^x$ (see Appendix B), the phase diagram in the (L', T) plane is identical to that of Fig. 3: We find either a single (first- or second-order) transition in P and P' , or a second-order transition in P followed, at a lower temperature T_P , by a first- or second-order transition in P' (see Fig. 6). Consequently we have found here a situation where the orientation of the principal axes of the quadrupoles is temperature dependent (see Ref. 16 for a discussion of this point), the dependence being continuous (see Fig. 7). In the case of a single transition just below T_D , one has $|P| \ll |P'|$ and $Q = c^{t\theta}$, so that $\tan 2\theta \approx 2\theta$ is proportionnal to P' .

In TbPO_4 there is only one crystallographic phase transition. We have two experimental informations: $T_D = 3.5^\circ\text{K}$ and the saturation value θ_0 of θ .^{11,15} (We suspect indeed that dipolar ordering will take place along z' and not modify very much the orientation of the quadrupoles since $T_N \ll T_D$.) Consequently, we may choose the values of the interactions L and L' to reproduce T_D and θ_0 . Choosing, for instance, $\theta_0 = 40^\circ$ and $T_P = 3.5^\circ\text{K}$, we find $L \approx 0$, $L' = 3.1^\circ\text{K}$. An external

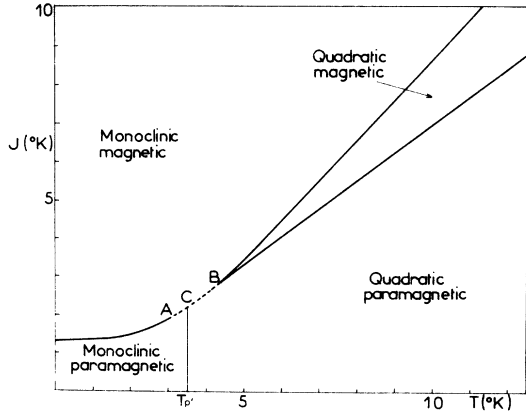


FIG. 8. Phase diagram in the (J, T) plane for Hamiltonian (10); $\Delta = 2.2^\circ\text{K}$ and $L' = 3.1^\circ\text{K}$. A and B are tricritical points. The dashed lines indicate first-order transitions.

magnetic field H_x would hinder or eventually suppress the monoclinic distortion, while a field H_z would on the contrary induce the distortion; H_x and H_z would also select some crystallographic domains.

Dipolar interactions may be added to Hamiltonian (9). In Sec. V we study the resulting Hamiltonian in the special case $L = 0$, and finally the full Hamiltonian ($L \neq 0$). Before going to Sec. V, we indicate a situation where three successive phase transitions are found. In Ref. 16 the following Hamiltonian was considered:

$$\mathcal{H} = -\Delta \sum_i Q_i - \sum_{ij} K_{ij} Q_i Q_j - \sum_{ij} L_{ij} P_i P_j.$$

For $\Delta < 0$, the following possibility was recognized for a range of values of K and L : a first-order transition in Q followed by a first-order transition in P . If the interactions

$$-\sum_{ij} J_{ij}^x S_i^x S_j^x$$

or

$$-\sum_{ij} L'_{ij} P_i P_j$$

are added to \mathcal{H} , a third transition in the parameter M_x (or P') is found.

V. TWO-PHASE TRANSITIONS IN TbPO_4

We study the Hamiltonian

$$\mathcal{H} = -\Delta \sum_i Q_i - \sum_{ij} L'_{ij} P_i P_j - \sum_{ij} J_{ij} (S_i^x S_j^x + S_i^y S_j^y). \quad (10)$$

We have taken $J_{ij}^x = J_{ij}^y = J_{ij}$ since it is known ex-

perimentally that the magnetic interactions in TbPO_4 are fairly well represented by a Heisenberg Hamiltonian.¹⁴ No interactions have been introduced between the y components of the spins and we did not look for magnetic ordering along y . If $J_{ij} = 0$, the spin density below T_p is represented by an ellipsoid whose principal axes are x' , y , and z' , and which is elongated mainly along z' so that, when $J_{ij} \neq 0$, we expect dipolar ordering to take place along or near z' .

The order parameters for the system are P' , M_z , and M_x . The phase diagram in the (J, T) plane is represented in Fig. 8 for $\Delta = 2.2^\circ\text{K}$ and $L' = 3.1^\circ\text{K}$. When J is small, a monoclinic distortion is followed at a lower temperature by a magnetic ordering in M_z and M_x . Along the line CB , the only transition is first order: The angle θ varies abruptly from zero to some finite value at the critical temperature. Beyond B , a second-order transition in M_z is followed at a lower temperature by a second-order monoclinic distortion which drives a rotation of the moments off the z axis. These results agree with the Landau theory. Magnetic ordering is described here by the two

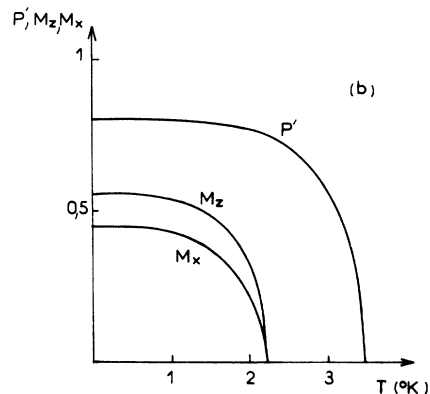
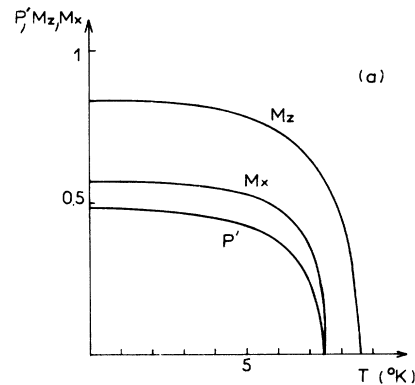


FIG. 9. Thermal variation of the parameters P' , M_x , and M_z according to Hamiltonian (10); $\Delta = 2.2^\circ\text{K}$, $L' = 3.1^\circ\text{K}$. (a) $J = 6^\circ\text{K}$; (b) $J = 1.5^\circ\text{K}$.

parameters S^x and S^z , which transform according to two different representations of the paramagnetic group, whence a single first-order transition or two successive second-order transitions.

For $J = 1.5^\circ\text{K}$, the quadrupolar transition in P' , at $T_{P'} = 3.5^\circ\text{K}$, is followed by a second-order dipolar transition in M_{xx} at $T_{M_{xx}} = 2.2^\circ\text{K}$ (see Fig. 9), in agreement with the experimental results. The thermal variation of the energy levels is shown in Fig. 10. The phase diagram of Fig. 8 shows that the magnetic transition might be of first order.¹⁴ The fact that the moments order along some direction of the xz plane and not along the x axis as found in Sec. III is a natural consequence of the monoclinic distortion of the crystal above the Néel temperature. This distortion must be very weak since it has not been detected by x-ray and neutron experiments,¹⁵ but is sufficient to create a strong anisotropy along z' . This anisotropy favors a spin-flip mechanism for metamagnetism, as shown by the ratio of critical fields along the two directions $[100]$ and $[001]$.¹¹

The occurrence of a crystallographic phase transition in TbPO_4 has been discovered only through a very careful measurement of the specific heat.¹³ Following the suggestion of Sec. IV one might reasonably ask whether there are in fact one or two crystallographic phase transitions, followed, of course, by a magnetic phase transition. Consequently we consider the general Hamiltonian

$$\mathcal{H} = -\Delta \sum_i Q_i - \sum_{ij} L_{ij} P_i P_j$$

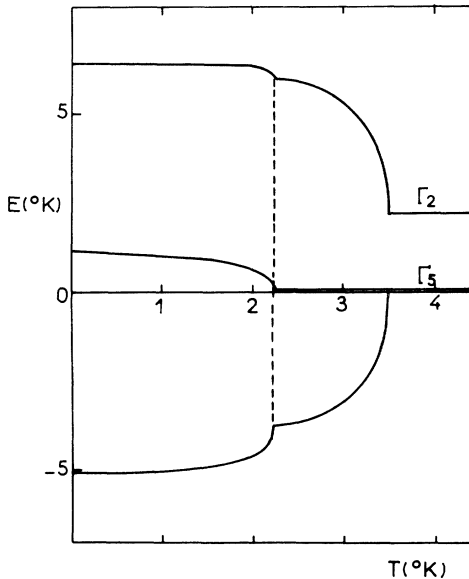


FIG. 10. Thermal variation of the single-ion energy levels according to Hamiltonian (10); $\Delta = 2.2^\circ\text{K}$, $L' = 3.1^\circ\text{K}$, and $J = 1.5^\circ\text{K}$.

$$- \sum_{ij} L'_{ij} P'_i P'_j - \sum_{ij} J_{ij} (S^x_i S^x_j + S^z_i S^z_j) \quad (11)$$

and we look for ordering in the parameters P , P' , M_x , and M_z and possibly for three successive phase transitions in P , P' , and M . We find, however, that, once the orthorhombic distortion is established, there is a competition between a monoclinic distortion and magnetic ordering along x , so that there are never more than two transitions: two crystallographic distortions (Sec. IV), an orthorhombic distortion followed by an ordering in M_x (Sec. III), or finally a monoclinic distortion (ordering in P and P') followed by an ordering in M_x and M_z (Sec. V), which seems to be the experimental situation. The following diagram summarizes the possible sequences of phase transitions in TbPO_4 :

$$\left(\begin{array}{l} \text{Paramagnetic} \\ \text{undistorted phase} \end{array} \right) \begin{array}{l} \rightarrow M_z \\ \rightarrow P \rightarrow M_x \\ \rightarrow P' \\ \rightarrow P, P' \rightarrow M_{xx} \\ \rightarrow P, P', M_{xz} \end{array}$$

VI. CRYSTALLOGRAPHIC DISTORTION IN TmAsO_4

The ground-state level of the Tm^{3+} ion in TmVO_4 is a Γ_5 doublet, and the first excited level is a singlet at 53.8 cm^{-1} , which is consistent with the result $g_1 \approx 0$ for the ground state. The crystallographic transition temperature is $T_D = 2.1^\circ\text{K}$ so that clearly the singlet plays no role in this transition, in agreement with the specific-heat measurements.⁵ Consequently the distortion of the lattice is orthorhombic or, more exactly, the monoclinic component of this distortion is negligible, since $\langle \Gamma_5 | S^x S^z + S^z S^x | \Gamma_5 \rangle = 0$.

On the contrary, in TmAsO_4 there is a low-lying excited singlet at about 14 cm^{-1} above the ground-state doublet,²¹ and in fact g_1 is large for the ground state.⁶ (The exact symmetry of the singlet is not known, but does not affect the form of the dipolar and quadrupolar operators determined for TbPO_4 in Sec. II.) Moreover, T_D is much larger than in TmVO_4 : $T_D = 6.1^\circ\text{K}$. TmAsO_4 cannot be represented by the doublet Γ_5 alone; possible couplings between the doublet and the singlet cannot be neglected. Such an interaction has been inferred from the specific-heat measurements²¹: Indeed the position of the singlet has been shown to be altered by the Jahn-Teller distortion. This result implies that the distortion is in fact monoclinic, as in TbPO_4 . Dipolar interactions must be weaker than the threshold value, so that no further magnetic transition is observed.

VII. GEOMETRICAL INTERPRETATION OF ABOVE RESULTS IN PYTTE AND STEVENS MODELS

We shall now interpret our results in terms of

the Pytte-Stevens model proposed for rare-earth vanadates.⁷ According to this model, in the high-temperature phase of DyVO₄ and TbVO₄, the moments may occupy four equivalent positions in the basal plane. Lowering the temperature reduces the number of these positions from four to two, which drives an orthorhombic distortion, then from two to one, which drives magnetic ordering in the basal plane. No monoclinic distortion is possible since the moments always lie in the plane. The same model applies to the arsenates TbAsO₄ and DyAsO₄.

Similarly in TbPO₄, TmVO₄, and TmAsO₄, we may postulate the existence of eight equivalent positions $[(\pm x, 0, \pm z)$ and $(0, \pm x, \pm z)]$ as discussed in Appendix C. Their number may be reduced from eight to four in the xz plane (TmVO₄), then from four to two $\pm(x, 0, z)$, and finally from two to one. The successive symmetries are then $\bar{4}2m \times 1'$; $2_x 2_y 2_z \times 1'$; $2_y \times 1'$; $2'_y$. The number of equivalent positions may also be reduced in one step from eight to two (TbPO₄, TmAsO₄) or one, or from four to one.

In the eight-position model, the total entropy variation is $\Delta S = R \ln 8$. We must then consider at least eight crystalline field levels of Tb³⁺ or Tm³⁺ to reproduce ΔS . In particular, we might use the whole crystal-field band defined by Trammel²² (in the present case $\Gamma_1 + \Gamma_2 + \Gamma_3 + \Gamma_4 + 2\Gamma_5$). If an effective spin $S' = 1$ is used to describe the system, that is, if only the three lowest levels ($\Gamma_5 + \Gamma_\alpha$) of the crystal-field band are considered, the exact entropy variation cannot of course be reproduced and it is not surprising that the maximum number of successive phase transitions is not found.

In DyVO₄ and TbVO₄ on the contrary, the whole crystal-field band (four levels) was considered, and it was possible to describe the maximum number (two) of successive phase transitions. The case of DyAsO₄²³ might be somewhat similar to that of TbPO₄, and it is discussed in Appendix D.

VIII. CONCLUSION

The crystallographic and magnetic phase transitions observed in TbPO₄ have been described phenomenologically. An axial symmetry-adapted spin Hamiltonian, exhibiting Jahn-Teller and magnetic interactions, has been constructed and treated in the molecular-field approximation. It has been found that if the paramagnetic distorted phase, which is stable between T_D and T_N , is orthorhombic, magnetic ordering appears necessarily along the x or y axis. Magnetic ordering takes place in fact off the c axis in the xz or yz plane and this situation can be explained only if the paramagnetic distorted phase is monoclinic, which implies a softening of the elastic constants c_{13} and c_{66} near T_D .

An elementary crystal-field calculation (Appendix C) has shown that, even in the undistorted paramagnetic phase, the Tb³⁺ moments have eight equivalent easy directions off the z axis. However, the possibility of three successive phase transitions has been discarded. This result does not contradict the Pytte-Stevens model, since only the low-lying levels of the crystal-field band have been considered.

The behavior of TmAsO₄ is very similar to that of TbPO₄, except that magnetic interactions are weaker, so that the onset of magnetic ordering is not possible.

ACKNOWLEDGMENTS

The author thanks J. Coing-Boyat, D. K. Ray, J. Rossat-Mignod, F. Sayetat, and F. Tcheou for helpful discussions.

APPENDIX A: CRYSTAL-FIELD PARAMETERS IN TbPO₄ AND TmAsO₄

The crystal-field Hamiltonian for rare-earth ions on a site of symmetry $D_{2d} = \bar{4}2m$ is

$$\mathcal{H}_c = \alpha V_2^0 O_2^0 + \beta (V_4^0 O_4^0 + V_4^4 O_4^4) + \gamma (V_6^0 O_6^0 + V_6^4 O_6^4).$$

The O_i^m operators are Stevens operators; the α , β , and γ coefficients depend on the rare-earth ion; the V_i^m coefficients are the crystal-field parameters which can be determined experimentally from the optical spectrum:

$$V_i^m = A_i^m \langle r^i \rangle.$$

The V_i^m have been determined for Er³⁺ diluted in YVO₄,²⁴ YAsO₄,²⁵ and YPO₄.²⁴ It is then possible to get approximate crystal-field parameters for other rare-earth ions if the average values $\langle r^i \rangle$ are corrected by interpolating the values computed for Kramers's ions by Freeman and Watson.²⁶ If these corrected parameters are used, crystal-field levels can be computed which are in reasonable agreement with the experimental spectrum, at least for the low-lying levels of TbVO₄, TbAsO₄, TmVO₄, and TmPO₄. The agreement is not so good for TbPO₄ and TmAsO₄: For TbPO₄, the calculated ground state is a Γ_5 , but the three first excited singlets are equidistant (the first excited singlet is a Γ_1); for TmAsO₄, the calculated

TABLE II. Transformation properties of the wave functions $|JM\rangle$ for $J=6$ in point group $D_{2d} = \bar{4}2m$.

Γ_α	$\bar{\mu}$	ν	$ M\rangle$
Γ_1	0	0	$ 0\rangle; 4\rangle + -4\rangle$
Γ_2	0	1	$ 4\rangle - -4\rangle$
Γ_3	2	0	$ 2\rangle - -2\rangle; 6\rangle - -6\rangle$
Γ_4	2	1	$ 2\rangle + -2\rangle; 6\rangle + -6\rangle$
Γ_5	± 1		$(\alpha 5\rangle + \beta 1\rangle + \gamma -3\rangle)$ $(\alpha -5\rangle + \beta -1\rangle + \gamma 3\rangle)$

TABLE III. Compatibility table for point groups $\bar{4}2m$, $2_x 2_y 2_z$, and 2_y .

$\bar{4}2m$	$2_x 2_y 2_z$	2_y
$\left. \begin{matrix} \Gamma_1 \\ \Gamma_3 \end{matrix} \right\}$	$\left. \begin{matrix} \Gamma_1 \\ \Gamma_2 \\ \Gamma_4 \end{matrix} \right\}$	Γ_1
Γ_5	Γ_3	
$\left. \begin{matrix} \Gamma_2 \\ \Gamma_4 \end{matrix} \right\}$	Γ_5	Γ_2

ground state is a singlet Γ_3 followed closely by a doublet Γ_5 , whereas the doublet is the experimental ground state (the symmetry-adapted wave functions are given in Table II).

In the case of $TbPO_4$ we tried to fit the five V_l^m parameters to the known part of the experimental spectrum (we used the results of Ref. 13, which disagree somewhat with those of Ref. 14). How-

TABLE IV. Transformation properties in groups $D_2 = 2_x 2_y 2_z$ and $C_2 = 2_y$.

			$(S^x)^2; (S^y)^2; (S^z)^2$	
D_2	Γ_1	A	$S^x S^y + S^y S^x$	$ 0\rangle_y$
	Γ_2	B_1	$S^x S^z + S^z S^x$	$ 0\rangle_z$
	Γ_3	B_2	$S^y S^z + S^z S^y$	$ 0\rangle_x$
	Γ_4	B_3	$S^x S^y + S^y S^x$	
C_2	Γ_1	A	$S^x S^y + S^y S^x$	$ 0\rangle_y$
	Γ_2	B	S^x, S^y	$ 0\rangle_x; 0\rangle_z$

ever, only the positions of the three first excited singlets are known, and the matrix elements of \mathcal{H}_c corresponding to the five V_l^m parameters are of the same order of magnitude, so that such a fit is not possible.

APPENDIX B: SYMMETRY CONSIDERATIONS

We first consider a true spin $S = 1$ in the symmetry $\bar{4}2m$. The representation D_1 of the rotation group is reducible according to $D_1 = \Gamma_2 + \Gamma_5$. The compatibility relations for the sequence of point groups $\bar{4}2m$, $2_x 2_y 2_z$, and 2_y is given in Table III. Transformation properties of the operators are given in Table IV.

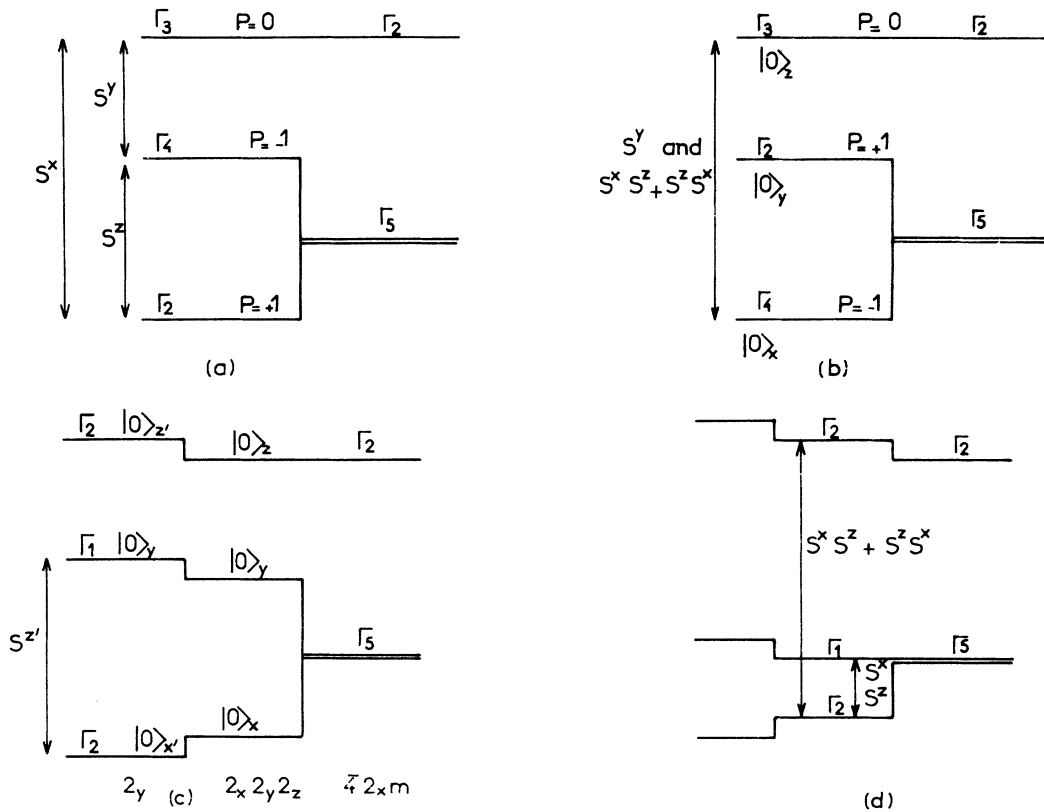


FIG. 11. (a) Energy levels of a spin 1 in the case of an orthorhombic distortion for the domains $P > 0$; (b) same as (a) but for $P < 0$; (c) successive orthorhombic and monoclinic distortions; (d) the experimental situation in $TbPO_4$.

In the case of an orthorhombic distortion, the ground-state wave function for the domain with $P > 0$ is $(|1\rangle + |-1\rangle)/\sqrt{2} = |0\rangle_y$ (the index y means that y is the quantification axis): In this state of symmetry Γ_2 , the spin density is mainly in the xz plane. For the domain with $P < 0$, the ground-state wave function is $(|1\rangle - |-1\rangle)/\sqrt{2} = |0\rangle_x$ and its symmetry is Γ_4 .

In Sec. III, we examined the possibility of an orthorhombic distortion followed by a magnetic transition; we selected the domain $P > 0$ and looked for ordering of the dipoles along x , neglecting the interactions $-J_{ij}^x S_i^y S_j^y$. Figure 2 shows that if P is positive, S^y indeed has no matrix elements connecting the ground state and some excited level, so that dipolar ordering along x is favored.

In Sec. IV, we considered again an orthorhombic distortion and the possibility of a further monoclinic distortion. We found in our numerical calculations that when P' is different from zero, P is negative, so that the monoclinic distortion in the $x-z$ plane is possible only for domains with a Γ_4 ground state ($P < 0$).

Comparison of Figs. 11(a) and 11(b) shows that the two situations examined above are similar once P is replaced by $-P$ and S^x by $S^x S^z + S^z S^x$. This explains the similarity of the phase diagrams in Figs. 3 and 6 and the fact that orderings in M_x and P' are competitive once the orthorhombic dis-

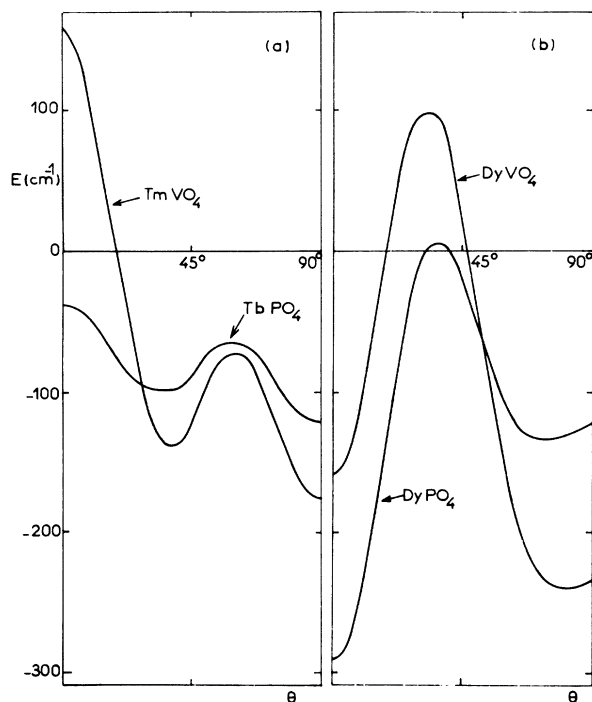


FIG. 12. Angular variation of the classical energy $E(\theta, \phi_0)$. (a) TbPO_4 and TmVO_4 ; (b) DyPO_4 and DyVO_4 .

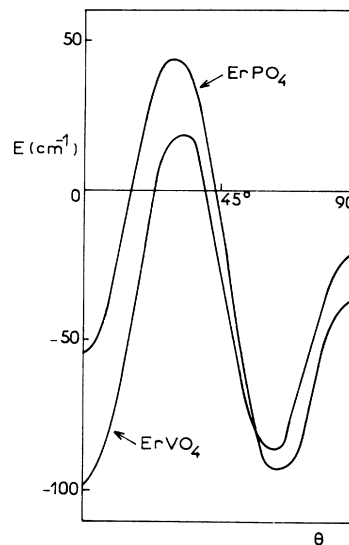


FIG. 13. Angular variation of the classical energy $E(\theta, \phi_0)$: ErPO_4 and ErVO_4 .

tortion is established, as stated in Sec. VI. Also, Table I shows that S^x and $S^x S^z + S^z S^x$ are orthogonal in the space of the Γ_5 representation.

Figure 11(c) illustrates successive orthorhombic and monoclinic distortions. In the axes x' , y , and z' , the point symmetry of the quadrupoles is orthorhombic and, as we checked by numerical calculation, the eigenstates are $|0\rangle_{x'}$, $|0\rangle_y$, and $|0\rangle_{z'}$. Finally, Fig. 11(d) illustrates the experimental situation.

Let us now consider an effective spin 1. The above considerations about the sign of P and the symmetry of the ground state in an orthorhombic phase do not hold since these two properties are not necessarily related to each other. For instance, in TbVO_4 ,³ the ground level separated from Γ_5 is Γ_4 when $P > 0$. However, the over-all discussion of this paper holds since the dipolar and quadrupolar operators we have used have been determined only by symmetry considerations.

APPENDIX C: JUSTIFICATION OF PYTTE-STEVENS MODEL

It is possible, knowing the five crystal-field parameters V_i^m , to calculate a classical expression of the crystal-field energy as a function of the orientation (θ, ϕ) of the magnetic moment:

$$\begin{aligned}
 E(\theta, \phi) = & \alpha V_2^0 J^2 (3 \cos^2 \theta - 1) \\
 & + \beta V_4^0 J^4 (35 \cos^4 \theta - 30 \cos^2 \theta + 3) \\
 & + \beta V_4^4 J^4 \sin^4 \theta \cos 4\phi \\
 & + \gamma V_6^0 J^6 (231 \cos^6 \theta - 315 \cos^4 \theta + 105 \cos^2 \theta - 5) \\
 & + \gamma V_6^4 J^6 \sin^4 \theta (11 \cos^2 \theta - 1) \cos 4\phi.
 \end{aligned}$$

We look for a minimum of $E(\theta, \phi)$. The term in V_4^4 is larger than the term in V_6^4 , so that if we choose $V_4^4 > 0$ (the sign of V_4^4 is not determined by the spectroscopic studies), $E(\theta, \phi)$ is minimum for $\phi_0 = 0$ (Tb, Er, Tm: $\beta > 0$) or $\phi_0 = 45^\circ$ (Dy, Ho: $\beta < 0$). It is sufficient then to compute $E(\theta, \phi_0)$. The minimum of $E(\theta, \phi_0)$ is found for $\theta = 90^\circ$ in the case of TbVO₄, TbAsO₄, DyVO₄, and DyAsO₄ and for $\theta = 0^\circ$ in the case of DyPO₄, in agreement with various magnetic measurements (Fig. 12). The difference between vanadates and phosphates is due to the difference in sign of V_2^0 .

In the case of TbPO₄, TmVO₄, TmAsO₄, and TmPO₄, a minimum of $E(\theta, \phi_0)$ is found for $\theta = 90^\circ$, but another minimum is found for $\theta_0 \approx 35^\circ$. In fact, g_{\parallel} and $g_{\perp} \neq 0$ in TmAsO₄; in TmVO₄, $g_{\perp} = 0$ for the ground state Γ_5 but this does not mean that the moments are along the c axis, since g_{\perp} is not characteristic of a whole crystal-field band. The relative values of the two minima should not be taken too seriously, since we used only approximate values of the crystal-field parameters for this calculation (see Appendix A). We think that the possibility of a monoclinic distortion in TbPO₄ and TmAsO₄ is a consequence of the existence of easy directions for the moments in the paramagnetic phase which are well off the c axis. Also, the value of θ_0 is in agreement with the neutron-diffraction results on TbPO₄.¹¹ The similarity between TbPO₄ and TmAsO₄ (or TmVO₄) lies in the fact that αV_2^0 has the same sign in the two compounds.

The fact that the moments in TbPO₄, TmVO₄, and TmAsO₄ are off the c axis could have been predicted from the consideration of the possible Trammel's crystal-field bands: If the moments are in the plane, as in TbVO₄, the crystal-field band is $\Gamma_1 + \Gamma_5 + \Gamma_3$; if they are along the c axis, the band is $\Gamma_1 + \Gamma_2$. The same remark applies to the three Er³⁺ compounds: If the moments are in the plane, the band is $\Gamma_6 + \Gamma_7$ as in DyVO₄ and DyAsO₄; if they are along the c axis, the band is made of a

doublet Γ_6 as in DyPO₄. The observed spectrum shows no well-defined band and the ground state is Γ_7 , so that the moments are off the c axis. This is in agreement with the classical picture (see Fig. 13) confirmed by the experimental values of g_{\parallel} and g_{\perp} for the ground state,²⁷ which are of the same order of magnitude.

APPENDIX D: DyAsO₄

According to the neutron-diffraction results,²² the moments lie 22° off the x axis in the xy plane and it is likely that their direction is fixed by the crystal field and not by the exchange interactions. Once more we may postulate the existence of eight equivalent positions for the moments: $(\pm x, \pm y, 0)$ and $(\pm y, \pm x, 0)$ with $\tan 22^\circ = y/x$. In DyAsO₄ the following sequence of phase transitions is found: The number of equivalent positions is reduced from eight to four, then from four to one, so that we have to describe ordering in $\langle S^x S^y + S^y S^x \rangle$ and then in $\langle (S^x)^2 - (S^y)^2 \rangle$ and $S^{x'}$ (x' being one of the principal axis of the quadrupoles in the xy plane below the second-ordering temperature). In Ref. 10 only four levels of the crystal-field band were introduced, as for the case of DyVO₄. Distortions along [100] and [110] are then competitive so that three successive phase transitions, and even the experimental situation, cannot be described unless the whole crystal-field band is introduced.

The above model, however, lies on the hypothesis that the easy direction of the moments in the xy plane are off the [100] or [110] axis. This is not possible if the point symmetry of the rare-earth site is $\bar{4}2m$, since the classical energy of the moments is then a function of $\cos 4\phi$. However, it becomes possible if the point symmetry of the site is only $\bar{4}$, the crystal-field parameter V_4^2 being different from zero, or if this parameter V_4^2 becomes different from zero in the orthorhombic phase as a morphic effect.

¹A. H. Cooke, D. M. Martin, and M. R. Wells, *Solid State Commun.* **9**, 519 (1971).

²H. G. Kahle, L. Klein, G. Müller-Vogt, and H. C. Schopper, *Phys. Status Solidi B* **44**, 619 (1971).

³K. A. Gehring, A. P. Malozemoff, W. Staude, and R. N. Tyte, *Solid State Commun.* **9**, 511 (1971); M. R. Wells and R. D. Worswick, *Phys. Lett. A* **42**, 269 (1972).

⁴W. Wüchner, W. Böhm, H. G. Kahle, A. Kasten, and J. Laugsch, *Phys. Status Solidi B* **54**, 273 (1972).

⁵A. H. Cooke, S. J. Swithenby, and M. R. Wells, *Solid State Commun.* **10**, 265 (1972).

⁶B. W. Mangum, J. N. Lee, and H. W. Moos, *Phys. Rev. Lett.* **27**, 1517 (1971).

⁷E. Pytte and K. W. H. Stevens, *Phys. Rev. Lett.* **27**, 862 (1971).

⁸R. J. Elliott, R. T. Harley, W. Hayes, and S. R. P. Smith, *Proc. R. Soc. A* **328**, 217 (1972).

⁹J. Sivardiere and M. Blume, *Phys. Rev. B* **5**, 1126 (1972).

¹⁰J. Sivardiere, *Phys. Rev. B* **6**, 4284 (1972).

¹¹J. N. Lee, H. W. Moos, and B. W. Mangum, *Solid State Commun.* **9**, 1139 (1971); S. Spooner, J. N. Lee, and H. W. Moos, *Solid State Commun.* **9**, 1143 (1971).

¹²H. C. Schopper *et al.*, *Phys. Status Solidi B* **46**, K115 (1971).

¹³H. C. Schopper, *Int. J. Magn.* **3**, 23 (1972).

¹⁴W. Böhm *et al.*, *Phys. Status Solidi B* **54**, 527 (1972).

¹⁵J. Coing-Boyat and F. Sayetat (unpublished).

¹⁶J. Sivardiere, A. N. Berker, and M. Wortis, *Phys. Rev. B* **7**, 343 (1973).

¹⁷G. F. Koster, J. O. Dimmock, R. G. Wheeler, and H. Statz, *Properties of the Thirty-Two Point Groups* (M.I.T. Press, Cambridge, Mass., 1963).

¹⁸M. Blume, *Phys. Rev.* **141**, 517 (1966).

¹⁹H. W. Capel, *Physica (Utr.)* **32**, 966 (1966).

²⁰H. H. Chen and P. M. Levy, *Phys. Rev. Lett.* **27**, 1383 (1971); and *Phys. Rev. B* **7**, 4267 (1973).

- ²¹J. H. Colwell and B. W. Mangum, *Solid State Commun.* **11**, 83 (1972).
- ²²G. T. Trammel, *Phys. Rev.* **131**, 932 (1963).
- ²³W. Schäfer and G. Will, *J. Phys. C* **4**, 3224 (1971).
- ²⁴D. Kuse, *Z. Phys.* **203**, 49 (1967).
- ²⁵H. G. Kahle and L. Klein, *Phys. Status Solidi B* **42**, 479 (1970).
- ²⁶A. J. Freeman and R. E. Watson, *Phys. Rev.* **127**, 1058 (1962).
- ²⁷See, for instance, M. Dzionara, H. G. Kahle, and F. Schedewie, *Phys. Status Solidi B* **47**, 135 (1971).